Proc. Natl. Acad. Sci. USA
Vol. 77, No. 10, pp. 5894–5898, October 1980
Biophysics

Bacteriorhodopsin is an inside-out protein

(purple membrane/neutron diffraction/membrane protein)

D. M. ENGELMAN*† AND G. ZACCAI‡

*Medical Research Council Laboratory for Molecular Biology, Cambridge, England; and ‡Institut Laue–Langevin, Grenoble, 38042 France

Communicated by Frederic M. Richards, June 18, 1980

ABSTRACT **Neutron scattering is particularly useful when parts of a structure can be deuterated. From *Halobacterium halobium* we have obtained, by biosynthetic incorporation, purple membranes in which all of the valines or all of the phenylalanines are present in deuterated form. Difference Fourier techniques permit a general assessment of the distribution of valine and phenylalanine in projections of the purple membrane structure. These show that valine is distributed toward the periphery of a single bacteriorhodopsin molecule, whereas phenylalanine is distributed toward its center. We use the facts that the amino acid sequence is known and that much of it can be assigned to the α helices of the bacteriorhodopsin structure to interpret our results. Comparison of our maps with the distribution of valine and phenylalanine around α-helical perimeters establishes the distribution of other amino acids and leads to the conclusion that the charged and polar groups of the bacteriorhodopsin molecule tend to lie at the molecular interior, away from contact with lipid, while the nonpolar surfaces are directed outward, making contact with the lipid regions. Thus, the protein is "inside-out" compared with the organization of soluble proteins.**

Halobacterium halobium is an organism that lives in environments containing high concentrations of salt (1). When oxygen supplies become limited, the organism synthesizes a specialized region of the plasma membrane that converts energy from visible light into stored energy by pumping protons across the plasma membrane (2, 3). This specialized region, the purple membrane, was discovered as a stable structure in isolation procedures at low ionic strength (4, 5). The membrane contains a single species of polypeptide to which is attached the prosthetic group retinal, which led to the use of "bacteriorhodopsin" as the name for the protein. It was also observed (6) that the protein exists in a two-dimensional crystalline lattice in the membrane. The protein remains stable for long periods at room temperature and is substantially unaffected by changes in hydration or the ionic strength of the environment. The features of stability and crystallinity have permitted a more detailed structural analysis than for any other integral membrane protein.

Two of the major advances in understanding this structure have come from electron microscopy and amino acid sequence analysis. By combining real space imaging and diffraction measurements in the electron microscope, Henderson and Unwin (7) combined information from a series of tilted specimens to obtain a three-dimensional density map at 7-Å resolution. The bacteriorhodopsin molecule was seen to contain seven rods of density extending through the membrane; these have been interpreted as α helices on the basis of their dimensions and packing.

To progress in understanding to the level of functional analysis and chemical detail, an essential step is knowledge of the amino acid sequence of bacteriorhodopsin. Recent reports describe the successful conclusion of years of effort to determine it (8, 9). The agreement of these reports with other, independent studies (10) provides confidence that the sequence is substantially correct. Together with the sequence information, useful data concerning the location of proteolytic cleavage points on the bacteriorhodopsin molecule were reported in these studies. Because the rods of density observed in the three-dimensional electron microscopic study lend themselves to interpretation as segments of α helix, it became of interest to attempt to fit the bacteriorhodopsin sequence information into a series of α-helical segments. Ovchinnikov and his colleagues have proposed one such organization (8). Engelman *et al.* (11) have refined this approach to identify seven α-helical regions in the sequence and to place these helical regions in the appropriate densities of the electron microscope map. Such model-building studies serve to frame the structural issues in a useful way and provide choices for the structure.

In an effort to provide tests for ideas concerning the distribution of amino acids in the structure, we have initiated neutron scattering experiments to map the general position of individual amino acid species in the projected view of the bacteriorhodopsin molecule. Our approach is based on the fact that hydrogenated and deuterated amino acids scatter neutrons quite differently. We have exploited the biosynthetic incorporation of deuterated amino acids by the organism to produce purple membrane preparations in which a single amino acid species is selectively deuterated. Neutron analysis then gives the distribution, in projection, of the amino acid in question, and it is possible to interpret the general features of such difference maps by using the assignments developed from model-building approaches to the α-helical regions of the protein. The interpretation of our preliminary maps shows that the polar amino acids in the α-helical regions are grouped toward the center of the protein molecule and the nonpolar residues in the α helices are on the protein surface in contact with membrane lipids. Thus, the protein is inside-out when compared with the organization of soluble proteins.

MATERIALS AND METHODS

Halobacterium halobium, strain S9, was grown on a defined medium with the following composition: NaCl, 250 g; $MgSO_4 \cdot 7H_2O$, 20 g; KCl, 2 g; sodium citrate, 3 g; $FeSO_4 \cdot 7H_2O$, 0.27 g; $CaCl_2 \cdot 6H_2O$, 0.5 g, KH_2PO_4, 0.2 g; NH_4Cl, 0.5 g; glycerol, 5.0 g; amino acid mixture or Oxoid L37 peptone, 7.5 g; and water to 1 liter. The pH of the medium was adjusted to 7.0 with sodium hydroxide solution. This medium is Newbold's

The publication costs of this article were defrayed in part by page charge payment. This article must therefore be hereby marked "*advertisement*" in accordance with 18 U. S. C. §1734 solely to indicate this fact.

† Present address: Department of Molecular Biophysics and Biochemistry, Yale University, P.O. Box 6666, New Haven, CT 06511.

modification (12) of the medium of Sehgal and Gibbons (13). For preparation of purple membranes without deuterated amino acids, the above medium with the peptone supplement was used. In cases where incorporation of a deuterated amino acid was desired, a defined mixture of pure amino acids was substituted for the peptone. This mixture had the following composition, in mg/liter: L-alanine, 215; L-arginine hydrochloride, 400; L-cysteine, 50; L-glutamic acid, 1300; glycine, 60; L-isoleucine, 220; L-leucine, 800; L-lysine hydrochloride, 850; L-methionine, 185; L-phenylalanine, 130; L-proline, 75; L-serine, 305; L-threonine, 250; L-tyrosine, 200; and L-valine, 500. This medium is based on that of Onishi *et al.* (14).

Cultures were grown to stationary phase at 37°C with controlled illumination and aeration. Purple membranes were isolated from washed cells by following the method of Oesterhelt and Stoeckenius (2).

In order to test for incorporation of single amino acids supplied in the medium, combined amino acid and radioactive analysis was used. Tritiated amino acids were used as tracers, and the distribution of radioactivity versus ninhydrin staining in fractions from the Durrum amino acid analyzer was determined after 24-hr hydrolysis of purple membrane in 6 M HCl. In the case of the amino acids used here, valine and phenylalanine, incorporation levels were high (see below) and metabolic transfer of ^3H to other individual amino acids was less than 1%.

Multi-layered specimens were prepared by drying suspensions of purple membrane (40 mg/ml) on an acid-washed glass coverslip. The drying was carried out at a slow rate, about 20 mg of membranes being deposited over an area of 8 cm^2. ω scans in the neutron diffractometer showed that such preparations have a mosaic spread of approximately 20° full width at half maximum.

Neutron measurements were carried out according to the method of Zaccai and Gilmore (15), using the D-16 diffractometer at the Institute Laue–Langevin in Grenoble. This instrument, which is similar in design to that of Nunes (16), consists of a set of collimating Soller slits that direct neutrons of 4.6-Å wavelength ($\Delta\lambda/\lambda = 1\%$) through the sample mounted with the planes of the membranes perpendicular to the incident beam. A second set of Soller slits set at an angle of 2θ to the direction of the collimating slits allows neutrons scattered at a narrow range (±0.1°) to strike the ^3He detector. Data were collected in ω, 2θ scans. The sample was maintained at 25°C and 84% relative humidity (H_2O).

Integrated intensities were obtained by subtracting a linear background from the observed reflection intensities. For overlapped reflections the intensity ratios from the electron microscope observations of Unwin and Henderson (17) were used. Thus, for example, the overlapped 3,4 and 4,3 would be divided in proportion to the observed electron microscope intensities for these reflections. After the assignment of intensities to individual reflections, the intensities were corrected by $[h^2 + k^2 + hk]^{1/2}$ and by a disorientation correction that is based on the variation of intensity along each lattice line as a function of tilt. This latter correction was determined from the variations seen in electron microscopy (R. Henderson, personal communication) and takes into account the observed mosaic spread of the specimen. The structure factors used in Fourier calculations were then obtained as the square root of the corrected intensities.

Phases observed in the electron microscope were used for Fourier calculations. It is felt that this is a reasonable procedure because the relative distribution of density is similar for neutrons and electrons at low resolution (7 Å). Fourier maps were calculated for the native and derivative structures. Difference Fourier maps for the deuterated valine and deuterated phenylalanine substitutions were also calculated; in these maps the structure factor for the deuterium-labeled membrane minus the structure factor for the native membrane was used as the Fourier coefficient. The difference maps were scaled by integrating the areas of protein and lipid density in Fourier maps of the native and derivative structures and scaling to obtain the difference of protein and lipid density expected for the total cross sections of the components in each sample.

RESULTS

An essential step in the design of the experiments described here is the incorporation of amino acids containing deuterium directly from the growth medium into the purple membrane. To explore the incorporation of valine and phenylalanine, defined media containing either amino acid in tritiated form were used in a series of growth studies. The purple membrane resulting from the growth was isolated and hydrolyzed, and its amino acids were separated in an amino-acid analyzer. The peaks detected in the analyzer were collected separately and assayed for radioactivity. The labeled amino acid used to supplement the medium was used as a standard for specific activity after a similar run on the analyzer. Experiments were conducted using valine and phenylalanine at different levels of supplementation in relation to the full supplement level described in *Materials and Methods*. The results of this analysis are shown in Table 1.

It is clear that high levels of incorporation are obtained with respect to specific activity. Less than 5% of the specific activity of the standard was found in any other amino acid species in the case of valine or phenylalanine incorporation. The high level of incorporation of valine is not surprising in light of the finding that valine is an essential amino acid (14).

On the basis of the successful incorporation studies, cells were grown, using deuterated valine and deuterated phenylalanine. From these cultures, a 100-mg sample of purple membrane containing deuterated valine and a 60-mg sample of purple membrane containing deuterated phenylalanine were obtained. Additionally, a 250-mg sample of native purple membrane was prepared, using the peptone medium described above. Each of these samples was dried on glass coverslips and diffraction experiments were conducted, using the D 16 neutron diffractometer according to the procedures of Zaccai and Gilmore (15). A total of 2 weeks of data collection led to the diffraction profiles shown in Fig. 1.

The native membrane gave a well-defined diffraction pat-

Table 1. Incorporation of ^3H-labeled amino acid from growth medium by purple membrane

Amino acid	Specific activity cpm/nmol	Specific activity % of standard
Valine standard	0.93	100
Valine supplement, 125 mg/liter	0.63	68
250 mg/liter	0.77	83
500 mg/liter	0.86	92
Phenylalanine standard	4.39	100
Phenylalanine supplement, 13 mg/liter	1.37	31
26 mg/liter	2.79	64
130 mg/liter	4.70	107

Specific activities are shown for amino acids derived from purple membranes after growth in a medium supplemented with different amounts of the standards shown.

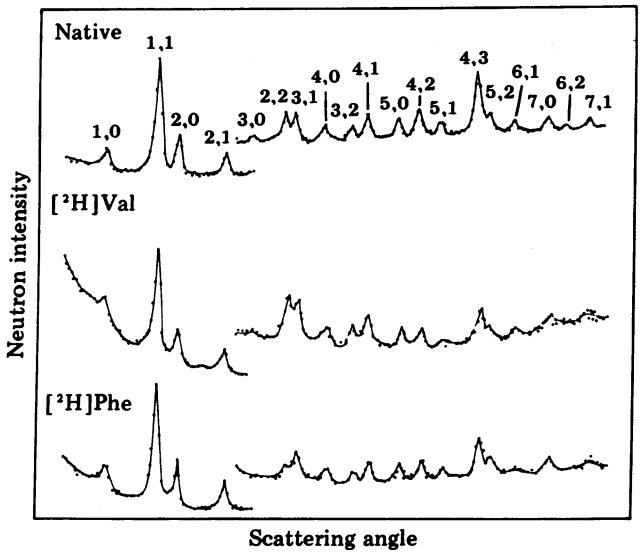

FIG. 1. Neutron scattering data are shown for native purple membranes and purple membranes containing deuterated valine or deuterated phenylalanine. Data are scaled approximately to the 1,1 reflection. Beyond the 2,1 reflection, the scales are expanded by a factor of 2. Sample sizes were 250, 60, and 100 mg for native, [²H]valine and [²H]phenylalanine, respectively. The difference in sample sizes accounts in part for the different relative contributions of direct beam background at small angles. It is also possible that some contribution in this region is due to the deuteration of part of the membrane structure.

tern containing 19 independently measurable peaks. The intensities corresponding to these peaks were treated according to the protocol described in *Materials and Methods* and a Fourier map was obtained. This map is shown in Fig. 2. It is apparent that the division of intensities and the phases used produce a map similar to that obtained by using data from the electron microscope (17).

The intensity distributions shown in Fig. 1 for the deuterated valine and deuterated phenylalanine-enriched purple membranes reveal several altered features. Although they are not so well measured as the native data set, it is apparent that many intensity changes have occurred. For example, compare the ratio of the 5,0 and 4,2 reflections between the deuterated valine and native data sets, and compare the ratio of the 2,2 and 3,1 reflections between the deuterated phenylalanine and native data sets. The mean change in structure factor ($\sum|F_{2H} - F_{1H}|/\sum F_{1H}$) was 0.13 for the phenylalanine data and 0.24 for the valine data.

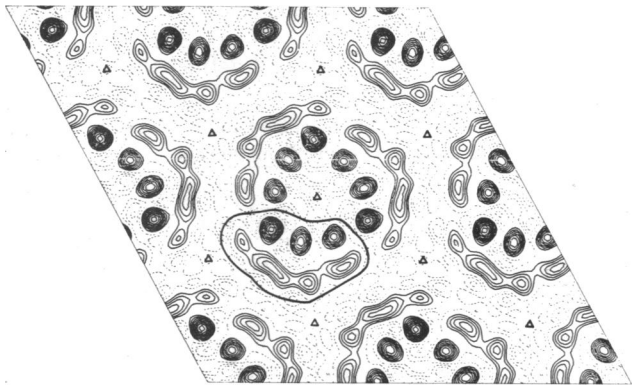

FIG. 2. Fourier map of the purple membrane seen in projection. The map was obtained by using the neutron structure factors obtained by dividing the intensity of each overlapped reflection in Fig. 1 according to the ratio found in electron microscopic studies and by using the phase for each reflection obtained in the same studies (17). The P_3 symmetry of the lattice is evident, and three molecules of bacteriorhodopsin are seen in the central portion of the map. An approximate outline for a single molecule has been added to guide the eye in this and subsequent maps. The zero-level contour has been omitted for clarity, and negative contours are shown as dashed lines.

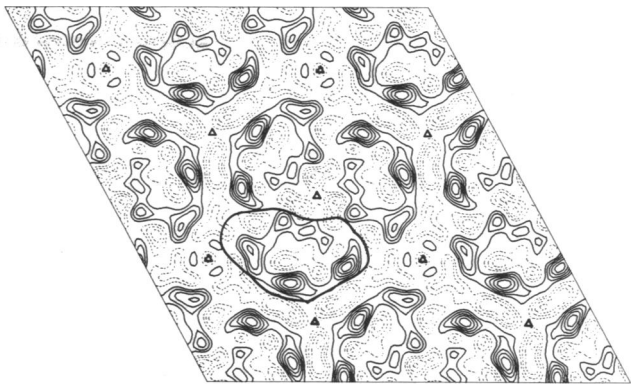

FIG. 3. Difference Fourier map comparing the native and deuterated valine-containing structures. Positive contours indicate the presence of regions rich in deuterated valine, and the zero-level contour is omitted. It is seen that the positive density lies within the same boundary indicated in Fig. 2 as the approximate periphery of a single bacteriorhodopsin molecule. The region toward the bottom of the molecule, which contains four tilted α-helical segments, contains the majority of the valine density. It is also evident that the density is near the periphery of the molecule, tending to lie on the outside surfaces of the α helices seen in projection in Fig. 2.

Difference Fourier maps were calculated for the deuterated valine and deuterated phenylalanine membranes in comparison with the native membrane in order to obtain some idea of the distribution of deuterated material in the bacteriorhodopsin molecule. Fig. 3 shows the distribution of valine in the membrane. It is apparent that the majority of positive density occurs within the bacteriorhodopsin molecule boundary, as it should. The density tends to be located at the periphery of the molecule, outside of the axes of the α helices. Much more density is apparent on the side of the molecule containing the four tilted helices than on the side of the molecule containing the three helices that are seen clearly as isolated densities in Fig. 2. This results in the appearance of a large region at the center of the molecule in which no positive contribution from deuterated valine is apparent.

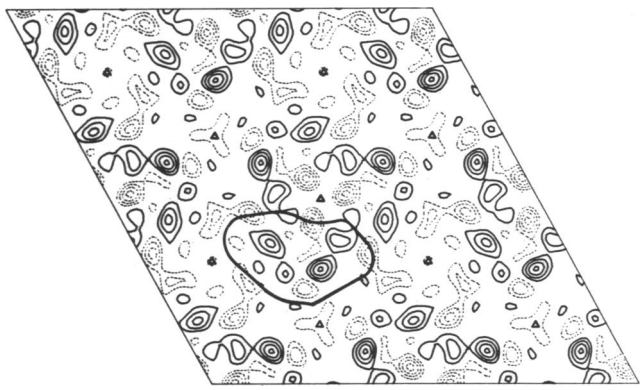

FIG. 4. Difference Fourier map showing the location of deuterated phenylalanine. Positive contours indicate the location of regions rich in deuterated phenylalanine and negative contours are shown as dashed lines. Again, the zero-level contour has been omitted for clarity. It is clear that the majority of positive density lies near the center of the bacteriorhodopsin molecule indicated by the dark line as in Fig. 2.

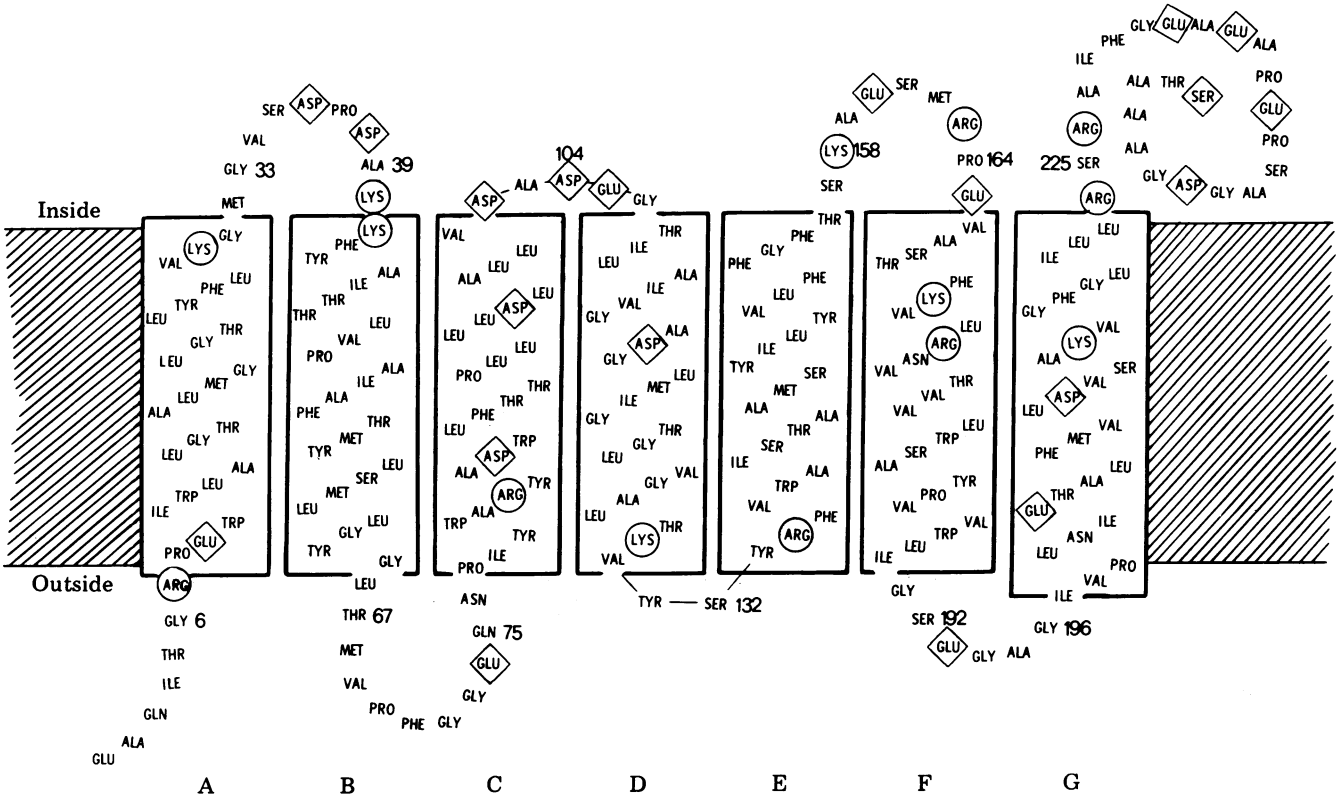

FIG. 5. Suggested arrangement of the bacteriorhodopsin polypeptide across the membrane. The seven helices are labeled A–G, starting from the amino terminus. The sequence is from Ovchinnikov *et al.* (8). The hatched areas indicate the approximate location of the lipid hydrocarbon regions. The retinal chromophore is bound through a Schiff base to lysine-41. ○ and ◇ indicate positive and negative charges, respectively. This figure is from Engelman *et al.* (11).

The deuterated phenylalanine maps, shown in Fig. 4, reveal a rather different distribution. Again, the principal positive density lies within the protein molecular boundary, as it should, but the major peaks of positive density are now located toward the interior of the protein molecule, on the inside of the α-helical axes, in contrast to the case with deuterated valine.

In assessing the validity of the difference maps, it is important to recognize the existence of four principal sources of error: counting statistics, the use of electron phases, the division of overlapped intensities, and the difference Fourier approximation for acentric structures. Noise from counting statistics has been studied by calculating maps using structure factors weighted by $1/\sigma^2$, and the major features are unaltered. Furthermore, the valine experiments have been repeated with new material and similar maps were obtained. With respect to the use of electron phases, experience has shown that our approximation is a good one at low resolution. The similarity between the intensity distributions for electrons and neutrons supports this view. The consequences of dividing overlapped reflections are less well defined. Model calculations by P. Rogan and G. Zaccai (unpublished) have shown that such a division procedure produces less noise in purple membrane difference maps than arises as a direct consequence of the failure of the difference Fourier approximation for acentric structures. Although each of these sources of error will contribute, the most serious source of noise in our maps appears to be inherent in the difference Fourier method, in which the phases of the native structure are assigned to the difference amplitudes. Because an isomorphous derivative of an acentric structure will, in general, produce phase changes, a noisy map containing negative excursions is expected. Nonetheless, the major features of such maps should be reliable. The facts that positive density in the difference maps is confined to the protein and that the two independent maps give rather different distributions that are consistent with ideas about the chemistry of the structure are indications of the validity of the maps. It is, however, appropriate to be restrained in detailed interpretation.

DISCUSSION

In order to understand the implication of the difference maps shown in Figs. 3 and 4, it is necessary to consider models for the distribution of amino acids in the α-helical regions of the bacteriorhodopsin structure. By combining the structural map of Henderson and Unwin (7) with the sequence data of Ovchinnikov *et al.* (8), assignments of α-helical regions shown in Fig. 5 have been made (11). For our interpretations, we assume the correctness of these helical assignments. Projections of the seven helices as seen in end-on views from the inside of the membrane are shown in Fig. 6. For each helix, four amino acid distributions are shown. The top row shows the distribution of valine in projection, the next the distribution of phenylalanine with each helix in the same rotational orientation as the top row, the third shows the distribution of potentially charged amino acid side chains that are located inside the membrane, and the bottom row shows the distribution of other polar amino acids. In a given column, the rotational orientation of a given helix is preserved, valine being arbitrarily oriented toward the top of the figure. It is apparent from the general distribution that the valine is largely located on the surfaces of the α helices that are opposite to the phenylalanine-rich surfaces, and that the charged and polar residues tend to be on the opposite surface from the valine and on the same surface as the phenylalanine. The observation from Figs. 3 and 4 that the valine density tends to be toward the outside of the bacteriorhodopsin molecule and that the phenylalanine density tends to be at the interior is consistent with the tendency of valine and phenylalanine to

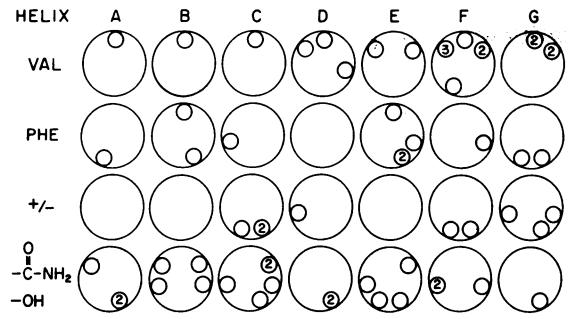

FIG. 6. The helical regions identified in Fig. 5 are shown in end-on projection as seen from the inside surface of the membrane. In each case, the orientation of helices A–G is maintained down the chart to show the location of valine, phenylalanine, charges, and polar groups, respectively. For example, helix G contains four valine residues, which have been assigned arbitrarily to the top of the helix projection as seen in the top row of the chart. Retaining the same orientation and moving down to the row labeled phenylalanine, we see that the two phenylalanine moieties in this helix are located almost exactly opposite to the valines. Further, the next line shows that the charged residues in helix G lie on the same side of the helix as phenylalanine and the opposite to valine. The corresponding view shown on the lowest line shows that the polar moiety lies opposite to valine and on the same side as phenylalanine and the charges. With the exception of helix B, all helices that contain both valine and phenylalanine have the majority of these amino acids on opposite faces of the helix. Those helices that contain charges that do not contact the aqueous regions on either side of the membrane have those charges on opposite faces to the valine-rich surface (C, D, F, and G). The uncharged polar residues also tend to be on the opposite side from the valine-rich surface and to coincide with the phenylalanine-rich charge-rich side of the helices.

occupy opposite sides of the α helices in our assignment. As a consequence of the model in Fig. 5, the polar and charged side chains can then be placed, in general, toward the interior of the molecule and the nonpolar surfaces of the α helices toward the exterior. The outer surfaces of the helices are remarkably nonpolar, as might be expected for a protein making contact with the hydrocarbon phase of a lipid bilayer. The interior of the protein, in this interpretation, is remarkably polar, containing many potentially charged groups and polar side chains. If we use the sequence data of Gerber *et al.* (9), no important changes of interpretation result. It has been suggested that the charged residues must act to form ion pairs (11), and the observed orientation of helices to place these residues toward the interior supports this point of view. It has also been suggested (18) that a succession of hydroxyl groups might participate in proton channels to and from the pumping site in the protein. The finding that a large number of hydroxyl-containing side chains are oriented toward the interior of the protein encourages the view that they may interact in such a role.

One may speculate concerning the occurrence of charged amino acid side chains that may make ion pairs at the protein interior. If they are not required for the proton translocation mechanism (which remains to be established), an alternative function may be to stabilize the membrane protein structure. Hydrophobic forces, which act to maintain the globular conformation of soluble proteins, will have weaker effects in maintaining the integrity of a protein that is largely buried in a lipid bilayer. If we consider the contribution of such forces to stabilizing bacteriorhodopsin against fluctuations in the plane of the membrane, they will contribute only insofar as the total surface area of the protein is increased by, for example, separating two of the α helices from the rest and inserting lipid molecules in between. The weak stabilization of the protein structure in this direction is due to the replacement of water by the hydrophobic phase of the lipid bilayer over a substantial proportion of the surface of the membrane protein. To compensate for the absence of such lateral stabilization, the use of ion pairs creating strong interactions between helices may be essential in order to provide a sufficiently stable structural environment for the controlled unidirectional translocation of protons. It may be that a similar structural motif will be found when other membrane proteins that are substantially embedded in membrane interiors are understood at a chemical level.

We believe that it would be premature to attempt a detailed interpretation of the distribution of valine and phenylalanine in terms of the identity of the different helices; however, the valine difference map suggests that helices F and G, the most valine-rich helices, are located in the region containing four tilted helices seen as a band of density in the lower part of the molecule outlined in Fig. 1.

To summarize, we find that the difference Fourier maps that locate deuterated neutrons of phenylalanine and valine in the bacteriorhodopsin molecule lead to the conclusion that the protein is inside-out compared with the normal distribution of polar and nonpolar amino acids found in soluble proteins. Within the membrane, the charged and polar residues are found distributed on the faces of the α helices that are directed toward the protein interior, and the external faces of the α helices are extremely nonpolar where they contact the interior of the lipid bilayer.

We thank R. Henderson, J. Walker, and D. Gilmore for discussions, and J. Jubb and K. Edwards for technical assistance. D.M.E. is grateful to the Medical Research Council Laboratory, the Institute Laue–Langevin, and the J. S. Guggenheim Foundation for sabbatical support. This work was supported in part by Grant PCM 78-11361 from the National Science Foundation and by Grants GM 22778 and HL 14111 from the National Institutes of Health.

1. Larsen, H. (1967) *Adv. Microbiol.* **1**, 97–132.
2. Oesterhelt, D. & Stoeckenius, W. (1971) *Nature (London) New Biol.* **233**, 149–152.
3. Oesterhelt, D. & Stoeckenius, W. (1973) *Proc. Natl. Acad. Sci. USA* **70**, 2853–2857.
4. Stoeckenius, W. & Rowen, R. (1967) *J. Cell Biol.* **34**, 365–393.
5. McClare, C. W. F. (1967) *Nature (London)* **216**, 766–771.
6. Blaurock, A. & Stoeckenius, W. (1973) *Nature (London) New Biol.* **233**, 152–155.
7. Henderson, R. & Unwin, P. N. T. (1975) *Nature (London)* **257**, 28–32.
8. Ovchinnikov, Yu., Abdulaev, N., Fergira, M., Kiselev, A. & Lobanov, N. (1979) *FEBS Lett.* **100**, 219–224.
9. Gerber, G. E., Anderegg, R. J., Helihy, W. C., Gray, C. P., Biemann, K. & Khorana, H. G. (1979) *Proc. Natl. Acad. Sci. USA* **76**, 227–231.
10. Walker, J. E., Carne, A. F. & Schmitt, H. (1979) *Nature (London)* **278**, 653–654.
11. Engelman, D. M., Henderson, R., McLachlan, A. D. & Wallace, B. A. (1980) *Proc. Natl. Acad. Sci. USA* **77**, 2023–2027.
12. Newbold, C. (1978) Dissertation (Cambridge University, Cambridge, England), p. 26.
13. Sehgal, N. & Gibbons, N. E. (1960) *Can. J. Microbiol.* **6**, 165–169.
14. Onishi, H., McCance, M. E. & Gibbons, N. E. (1965) *Can. J. Microbiol.* **11**, 365–373.
15. Zaccai, G. & Gilmore, D. (1979) *J. Mol. Biol.* **132**, 181–191.
16. Nunes, A. C. (1973) *Nucl. Instrum. Methods* **108**, 189–191.
17. Unwin, P. N. T. & Henderson, R. (1975) *J. Mol. Biol.* **94**, 425–450.
18. Nagle, J. & Morowitz, H. J. (1978) *Proc. Natl. Acad. Sci. USA* **75**, 298–302.